ISSN 1573-160X, *PHYSICAL OCEANOGRAPHY*, Vol. 31, Iss. 5, pp. 679-693 (2024)

published in *Morskoy Gidrofizicheskiy Zhurnal*, 2024, Vol. 40, Iss. 5, pp. 723–737

Original article

Estimates of Available Potential Energy Budget in the Black Sea Using Different Schemes for Calculating Heat and Salt Advective Transport

O. A. Dymova

Marine Hydrophysical Institute of RAS, Sevastopol, Russian Federation
✉ *olgdymova@mhi-ras.ru*

Abstract

Purpose. The study is purposed at analyzing the available potential energy and its budget components in the Black Sea based on the results of numerical circulation modeling using a new temperature and salinity approximation scheme in the advective transport operator.

Methods and Results. Two numerical experiments were carried out based on the MHI model versions differing from each other in their approximation schemes of advective terms. The difference between the schemes is that in experiment 1, the condition of conserving temperature and salinity in the first and second degrees is satisfied, whereas in experiment 2 – temperature in the first and third degrees and salinity in the first and fifth degrees are conserved. It is found that application of the new scheme is accompanied by an increase in the available potential energy reserve by on average 30% over a year. The difference is conditioned by a decrease in both horizontal diffusion in a warm season and consumption of available potential energy through the buoyancy work in a cold season. The modeling results validated by the temperature and salinity measurement data from the MHI Oceanographic Data Bank show that application of the new approximation scheme permits to specify the density field and the energy characteristics in the Black Sea upper layer. Below the 300 m horizon, the discrepancies between the model and *in-situ* thermohaline fields in two experiments are minor, whereas the qualitative and quantitative distinctions in energy fields are significant: difference in the values of available potential energy in the basin central and periphery parts as well as the area of zones with the extreme buoyancy work values increase.

Conclusions. Application of the new approximation scheme of temperature and salinity in the advective transport operator makes it possible to specify the field density and, as a consequence, to obtain more accurate estimates of the available potential energy of sea circulation. In the Black Sea upper layer (the main pycnocline layer and above), the difference between the fields of energy characteristics calculated in two experiments is due to the differences in spatial distribution of density anomalies, at that the anomaly absolute values and the maximum energy values in the experiments are close in their magnitudes. Below the pycnocline layer, application of the new scheme is followed by the growth of available potential energy since the temperature and salinity changes lead to an increase in the gradients of density anomalies normal to the coast.

Keywords: Black Sea, modeling, circulation, available potential energy, buoyancy work, density anomaly, thermohaline characteristics

Acknowledgements: The study was carried out within the framework of the state assignment theme of FSBSI FRC MHI FNNN-2024-0001.

For citation: Dymova, O.A., 2024. Estimates of Available Potential Energy Budget in the Black Sea Using Different Schemes for Calculating Heat and Salt Advective Transport. *Physical Oceanography*, 31(5), pp. 679-693.

Introduction

Mesoscale eddy motions in the oceans and seas are one of the main mechanisms of vertical and horizontal matter and energy redistribution in marine water areas. According to classical concepts [1, 2], the formation of such eddies is associated with the release of some part of the ocean potential energy called the available potential energy (APE) and its transformation into eddy kinetic energy. The APE budget study makes it possible to estimate the role of the main physical forces in the mesoscale sea dynamics. Based on estimates of energy fluxes, it was shown in [3] that baroclinic production caused by the transfer of density anomalies by currents and potential and kinetic conversion determined by the vertical eddy flux of buoyancy force are the main mechanisms of APE transformation for the World Ocean. In [4], the results of a study of global eddy APE are presented and, in addition to [3], it is indicated that in the upper mixed layer of the ocean, diabatic mixing, atmosphere interaction at the water–air boundary and internal diffusion play a significant role in the APE budget. The literature also shows regional features of the APE distribution and evolution in large scale ocean currents. Thus, in [5], estimates of baroclinic conversion rate of APE were carried out and it was found that since it was an order of magnitude greater than the rate of barotropic conversion of eddy kinetic energy, it was this factor that explained the baroclinic nature of the Gulf Stream instability. In [6], it is shown that not the wind effect, but APE variations as a result of the thermal ocean–atmosphere interaction play a decisive role in the budget of eddy kinetic energy in the Kuroshio Extension region.

In modern conditions, numerical modeling is one of the main tools for diagnosing and predicting hydrodynamic and energy characteristics of circulation. Traditionally, the equations of the energy change rate are derived from the differential equations of ocean energy [3, 7], but their discrete analogues, which are not an exact consequence of the finite-difference equations of the ocean model, will introduce an error in the quantitative estimates of energy fluxes. In addition, to estimate APE correctly when moving from the difference equation of advection–diffusion of density to the equation of energy change rate, it is necessary to approximate the density adequately at those points of the difference template where it is not calculated directly. Taking into account the above considerations, a scheme for the approximation of the equation of APE change rate is proposed in [8]. It is obtained as a result of a strict algebraic transformation of the finite–difference equations of the model. In [9], a new scheme for the approximation of temperature and salinity on the cell edges is described (for a finite–difference template, where temperature and salinity are calculated at the cell center), which provides a divergent form of the density advection equation for an arbitrary polynomial dependence of density on temperature and salinity.

The present paper is an extended version of the report of the 14th International Conference “Waves and Vortices in Complex Media” 2023 [10] continuing the numerical analysis of the Black Sea energy [11]. To estimate how the scheme for calculating thermohaline characteristics affects the spatial and temporal variability

of energy fluxes that form APE, this paper includes a circulation modeling based on the approximations proposed in [8, 9]. All terms of the APE budget equation were calculated and analyzed and a comparison was made with previously obtained data.

Calculation method and data used

Analysis of the APE distribution features in the Black Sea is carried out using the example of circulation modeling in 2016. Numerical experiments were carried out using the eddy resolving model of Marine Hydrophysical Institute with a resolution of 1.6 km [11]. The model is constructed based on the complete system of equations of ocean thermohydrodynamics in the Boussinesq approximation and hydrostatics. The state equation is represented by a nonlinear dependence of density on temperature and salinity. Vertical turbulent mixing is parameterized by the Mellor–Yamada 2.5 closure model [12], horizontal diffusion in the heat and salt equations as well as horizontal viscosity in the equations of motion are described by the Laplace operator to the second degree with constant coefficients of the corresponding dimension. Wind stress, heat fluxes, precipitation and evaporation according to the ERA5 [1] reanalysis data are specified as boundary conditions on the free surface. On the solid lateral sections of the boundary, the conditions of equality to zero of the normal velocity and the normal derivative of the tangential velocity as well as the equality to zero of their Laplacians are set. The equality to zero of the normal derivatives and their Laplacians are set for the temperature and salinity. On the bottom, the no-slip condition and the condition of the absence of normal heat and salt fluxes are set. The model takes into account the climatic runoff of rivers and water exchange through straits [13] and Dirichlet conditions are set on the liquid sections of the boundary. Correction of inaccuracies in the specification of the heat flux from the atmosphere to the sea surface is carried out by assimilating the satellite sea surface temperature [14]. The basin bathymetry is constructed on the basis of the EMODnet digital depth array [2]. The finite–difference approximation of the model equations is carried out on grid C [15]. The complete physical formulation of the problem, the coefficients used and the parameterizations are presented in detail in [11].

Two numerical experiments on the circulation modeling and the exact calculation of the APE budget were carried out in the work. The difference between them is in the method of temperature T and salinity S calculating in the finite–difference operator of advective transport which, for example, has the following form for the temperature (similarly for salinity):

[1] Hersbach, H., Bell, B., Berrisford, P., Biavati, G., Horányi, A., Muñoz Sabater, J., Nicolas, J., Peubey, C., Radu, R. [et al.], 2018. ERA5 Hourly Data on Single Levels from 1940 to Present: Data Set. In: *Copernicus Climate Change Service (C3S) Climate Data Store (CDS)*. [Accessed: 25 June 2023]. https://doi.org/10.24381/cds.adbb2d47

[2] EMODnet. *EMODnet European Marine Observation and Data Network*. [online] Available at: https://doi.org/10.12770/ff3aff8a-cff1-44a3-a2c8-1910bf109f85 [Accessed: 27 August 2024].

$$ADV^T = \left[u_{i+1/2,j,k}\left(T_{i+1/2,j,k} - T_{i,j,k}\right) - u_{i-1/2,j,k}\left(T_{i-1/2,j,k} - T_{i,j,k}\right)\right]h_x^{-1} +$$
$$+\left[v_{i,j+1/2,k}\left(T_{i,j+1/2,k} - T_{i,j,k}\right) - v_{i,j-1/2,k}\left(T_{i,j-1/2,k} - T_{i,j,k}\right)\right]h_y^{-1} +$$
$$+\left[w_{i,j,k+1/2}\left(T_{i,j,k+1/2} - T_{i,j,k}\right) - w_{i,j,k-1/2}\left(T_{i,j,k-1/2} - T_{i,j,k}\right)\right]\left(h_z^k\right)^{-1},$$

where *u*, *v*, *w* are components of the current velocity vector; *h* is spatial step size in the corresponding direction; *i*, *j*, *k* are coordinates of the model grid nodes in the space of grid functions corresponding to the middle of the cell on grid C [16]. Since temperature, salinity and density on grid C are calculated at the center of the model cell [15], their values on the cell edges (half-integer indices) are, strictly speaking, unknown. It is shown in [9] that under adiabatic conditions and in the absence of external sources with a nonlinear equation of state independent of pressure, to preserve the discrete integral of density, it is advisable to use such approximations of the nonlinear terms on the cell edges so that along with *T* and *S*, T^m and S^l are preserved, where *m* and *l* are positive integers greater than 2. In experiment 1, the formula below was used to calculate *T* and *S* on the cell edges

$$T_{i+1/2,j,k} = \frac{T_{i+1,j,k} + T_{i,j,k}}{2},\ S_{i+1/2,j,k} = \frac{S_{i+1,j,k} + S_{i,j,k}}{2}, \qquad (1)$$

and the detailed derivation of the formula in experiment 2 is shown in [9]:

$$S_{i+1/2,j,k} = \frac{4}{5}\frac{S_{i+1,j,k}^4 + S_{i+1,j,k}^3 S_{i,j,k} + S_{i+1,j,k}^2 S_{i,j,k}^2 + S_{i+1,j,k} S_{i,j,k}^3 + S_{i,j,k}^4}{S_{i+1,j,k}^3 + S_{i+1,j,k}^2 S_{i,j,k} + S_{i+1,j,k} S_{i,j,k}^2 + S_{i,j,k}^3}, \qquad (2)$$

$$T_{i+1/2,j,k} = \frac{2}{3}\frac{T_{i+1,j,k}^2 + T_{i+1,j,k}T_{i,j,k} + T_{i,j,k}^2}{T_{i+1,j,k} + T_{i,j,k}}.$$

Formulas (1) and (2) describe the change in *T* and *S* along the *x* coordinate (for *y* and *z* similarly). For both calculation methods, the finite–difference operator of advective transport has the second order of approximation. The difference between the experiments is that *T*, *S* and T^2, S^2 were preserved in experiment 1 and *T*, *S* and T^3, S^5 in experiment 2. Approximation (2) has limitations at |T|≪ 1°C and/or |S|≪ 1‰. As for the Black Sea conditions, such a situation is practically atypical and it is not taken into account in the presented calculations.

The APE change rate was calculated using the following formula

$$\frac{\partial APE_{i,j,k}}{\partial t} + \left\{\delta_x\left(u_{i,j,k}a_{i,j,k}^{pe}\right) + \delta_y\left(v_{i,j,k}a_{i,j,k}^{pe}\right) + \delta_z\left(w_{i,j,k}a_{i,j,k}^{pe}\right)\right\}\left(\delta_z\rho_k^s\right)^{-1} =$$
$$= -g\,\overline{w_{i,j,k}}^z\rho_{i,j,k}^* + \omega_{i,j,k} + (D_H + D_V)_{i,j,k},$$

$$APE_{i,j,k} = a_{i,j,k}^{pe}(\delta_z\rho_k^s)^{-1},\quad a_{i,j,k}^{pe} = g\frac{\left(\rho_{i,j,k}^*\right)^2}{2}, \qquad (3)$$

where *APE* is APE density; δ is finite-difference analogue of the differentiation operator with respect to the corresponding coordinate; *g* is acceleration of gravity; $\rho^s$is average density of sea water over the area of the *k* layer; ρ^* is density anomaly calculated as the difference between the local and average density over the layer; D_H,

D_V are horizontal and vertical diffusion components of the APE budget; ω is designation of additional difference terms that have no analogue in the differential equation and result from the rigorous derivation of formula (3) from the finite-difference equations of the model. Note that ω includes terms that take into account the change in density anomalies on the cell edges and are associated with advective transport, and D is additional diffusion terms. The derivation and full form of the terms ω, D_H and D_V are presented in [8]. For ease of interpretation of the experimental results, equation (3) is rewritten in symbolic form:

$$\frac{\partial APE}{\partial t} = ADV + WRG + DIFH + DIFV,$$

where *ADV* is APE change due to advective transport, *WRG* – due to the buoyancy work, *DIFH* and *DIFV* – due to horizontal and vertical diffusion, respectively.

As a result of numerical experiments for each day of 2016, 3D fields of temperature, salinity, density, current velocity, density anomalies, APE field and its budget components were obtained. Validation of the results of thermohaline field modeling was carried out based on the data obtained from the MHI Oceanographic Data Bank [17]. Contact measurements of temperature and salinity were carried out by Argo profiling floats as well as during R/V *Professor Vodyanitsky* cruises in 2016. Table presents the root mean square deviations (RMSD) between the model and natural values of temperature and salinity for all available observational data. As can be seen from Table, in experiment 2, the RMSD of temperature in the 30–100 m layer decreases by 25%, and the average RMSD of salinity for horizons from 0 to 100 m decreases by 21%. The difference between the RMSD for the two experiments is insignificant for deep water horizons below 300 m.

Root mean square deviation between the model and *in-situ* temperature and salinity

Depth, m	Experiment 1		Experiment 2	
	Temperature, °C	Salinity, ‰	Temperature, °C	Salinity, ‰
0–5	0.79	0.28	0.94	0.22
5–30	1.53	0.23	1.54	0.17
30–100	1.12	0.67	0.84	0.56
100–300	0.26	0.48	0.27	0.50
300–800	0.05	0.09	0.07	0.10
800–1500	0.03	0.08	0.03	0.08

Comparison of the modeling results with *in-situ* data showed that the decrease in the RMSD in the upper 100 m layer of the Black Sea when using approximation scheme (2) from the point of view of practical hydrology was manifested in a decrease in the thickness of the upper mixed layer in the winter period and a decrease in the depth of the upper boundary of the thermocline layer in summer in the central part of the sea.

Results

Analysis of the integral and spatial distributions of the APE budget components and comparison with distribution of thermohaline and dynamic characteristics of circulation based on the results of numerical experiments were carried out. Both experiments started with the same initial conditions, and significant differences in the values of the model parameters appeared in April. It was found that, starting from spring, the volume-average APE in experiment 2 exceeded its values in experiment 1; this difference was about 30% on average per year. Since the Black Sea is characterized by strong seasonal variability of hydrophysical fields [18], summer (May–June) and winter (November–December) periods were considered for a more detailed comparison.

Fig. 1 shows the change in the volume-average *APE*, *WRG* and *DIFH* over time for two experiments in summer and winter 2016. Analysis of the change in the APE budget components over time showed that in summer season, the APE increase in experiment 2 (Fig. 1, *a*) was associated with energy loss decrease due to horizontal diffusion (Fig. 1, *b*). At the same time, the spatial distribution of the *DIFH* component indicates horizontal diffusion weakening in the coastal zone on the northwest shelf (NWS) and in the deep water part of the sea [10, p. 379, Fig. 1, *b*]. Analysis of the thermohaline characteristics on the NWS in experiment 2 revealed a decrease in horizontal salinity gradients which determines energy flux decrease due to horizontal diffusion. In the central part, the diffusion flux decreases due to a more uniform spatial distribution of the density field.

According to the mathematical formulation of the problem in the MHI model, a positive *WRG* value corresponds to the APE transformation into kinetic energy, i.e., its decrease. For the curves shown in Fig. 1, *d*, the average values of the $<WRG>_V$ parameter are $0.15 \cdot 10^{-5}$ and $0.01 \cdot 10^{-5}$ W for experiments 1 and 2, respectively. Thus, in winter, the increase in the APE store in experiment 2 (Fig. 1, *c*) is stipulated by a smaller amount of APE spent on transformation into kinetic energy. In addition, as shown in [10, p. 380, Fig. 2], the energy flux caused by the transformation of kinetic energy into available potential energy increases in the western and southwestern parts of the continental slope in experiment 2. The *WRG* component is determined by the density and vertical velocity. Therefore, cooling and intensification of winter convection are the main reasons for the increase in APE store in winter.

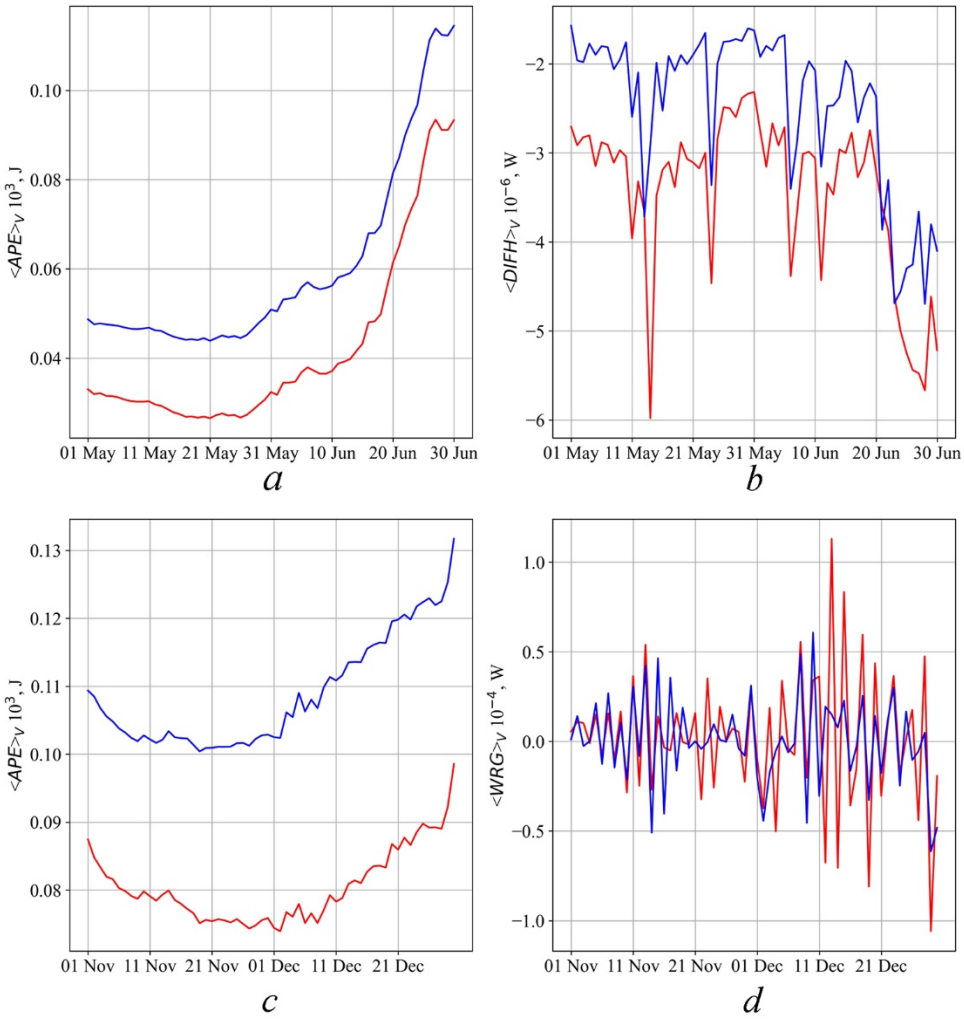

F i g. 1. Change over time of volume-average APE (*a*, *c*), horizontal diffusion of APE (*b*) and buoyancy work (*d*) for two experiments in May–June (*a*, *b*) and November–December (*c*, *d*) 2016. Red line is experiment 1, blue line is experiment 2

Comparison of the *APE* and *DIFH* curves in two experiments shown in Fig. 1 demonstrates the similarity of the temporal variability of the volume-average values of the energy characteristics. This behavior of the curves is probably due to the variability of external conditions. It was shown earlier in [19] that the upper 30 m sea layer most strongly affected by thermohaline forcing made maximum contribution to the APE store in the Black Sea. Since the boundary conditions for both experiments are the same, the variability over time of the average integral *APE* and *DIFH* values is almost identical in the experiments. The shift of the curves along the ordinate axis results from an increase in the average density anomaly due to changes in the thermohaline characteristics.

For summer and winter periods, the change in the APE store by depth was estimated for two experiments. For this purpose, the difference between the average

APE by volume of layer k in two calculations $\Delta APE_k = < APE_{\exp 2} >_{V_k} - < APE_{\exp 1} >_{V_k}$ was calculated in each model layer. A positive value of ΔAPE_k indicates that the APE store in layer *k* is higher in experiment 2. It was found that in summer, in the 5–40 m layer, the average APE was higher in experiment 1 (Fig. 2, *a*, curves 3–9). Starting from the 60 m horizon (Fig. 2, *a*, curves 11 and below), the APE in experiment 2 exceeds the values in experiment 1 reaching a maximum at layer 21 (Fig. 2, *a*, curve 21) corresponding to the 500–700 m depth.

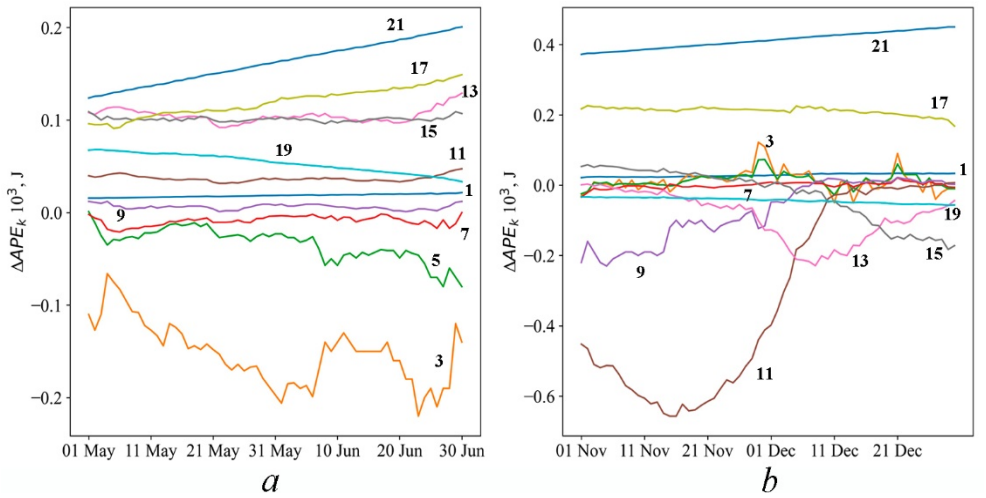

F i g. 2. Change over time of difference ΔAPE_k in May–June (*a*) and November–December (*b*) 2016. Numerals are the layer numbers (index *k*)

For winter season in the 40–100 m layer, the ΔAPE_k value is negative (Fig. 2, *b*, curves 9–13), therefore, the APE in the first experiment is higher than in the second one. For deep water horizons in winter, as well as in summer, the APE store in experiment 2 is higher than in experiment 1. However, the maximum difference between the calculations in winter is almost twice as large.

Discussion

Initial and boundary conditions for the numerical experiments were the same varying only in the scheme for calculating the temperature and salinity in the advective heat and salt transfer operator. No other changes to the finite–difference equations of the model or the values of the model constants were made. All the differences among the calculation results described above are directly or indirectly through a change in density due to a change in temperature and salinity advection. To determine the physical causes of the differences revealed, spatial distributions of the energy and hydrological characteristics of the circulation at different horizons in summer and winter periods will be considered in more detail. As shown above, in summer, the APE store in the upper sea layer is higher in experiment 1. Spatial distribution analysis of the APE density and local seawater

density anomaly in June shows that APE is smaller in the upper layer in experiment 2 (Fig. 3, *b*) due to the lower absolute values of the density anomaly on the NWS (Fig. 3, *d*) compared to experiment 1.

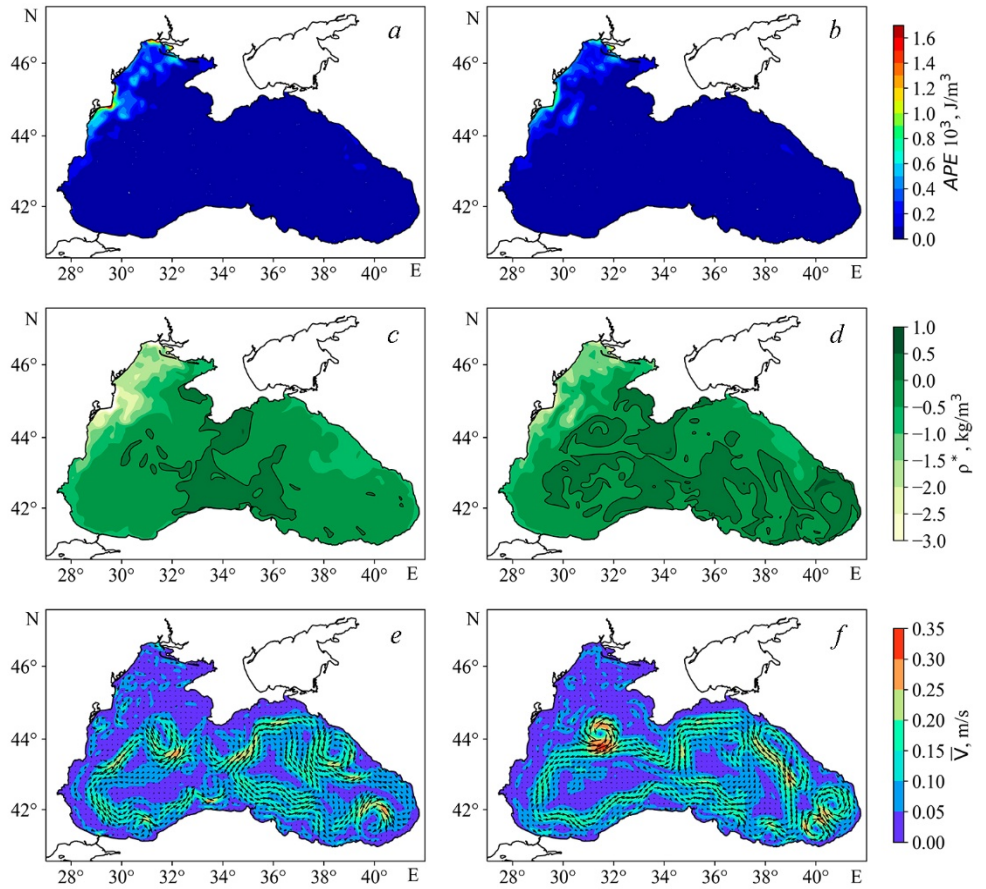

F i g. 3. Spatial distributions of *APE* (*a*, *b*), density anomaly (*c*, *d*) and current velocities (*e*, *f*) at the 5 m depth based on the results of experiments 1 (*a*, *c*, *e*) and 2 (*b*, *d*, *f*) on June 15, 2016

Decrease of the density anomaly module is due to lower temperature values and higher salinity compared to experiment 1. As can be seen from the results of the validation of thermohaline characteristics (Table), the use of the new approximation scheme (2) makes it possible to improve the reproduction of salinity in the upper 100 m layer. Since the density depends predominantly on salinity [20] in the Black Sea, it can be assumed that the density anomaly used in formula (3) was more correctly calculated in experiment 2. Consequently, the APE estimates obtained in experiment 2 are more realistic.

When comparing Figs. 3, *c* and 3, *d*, a difference in the area of positive density anomalies in the central part of the sea is observed, which has little effect on the APE spatial distribution, but shows similarity with the current velocity fields (Fig. 3, *e*

and *f*). Extensive positive anomalies correspond to denser waters within the Black Sea Rim Current in experiment 2 in summer indicating a more intense cyclonic circulation (Fig. 3, *f*) and upwelling of deep waters in the central part of the sea.

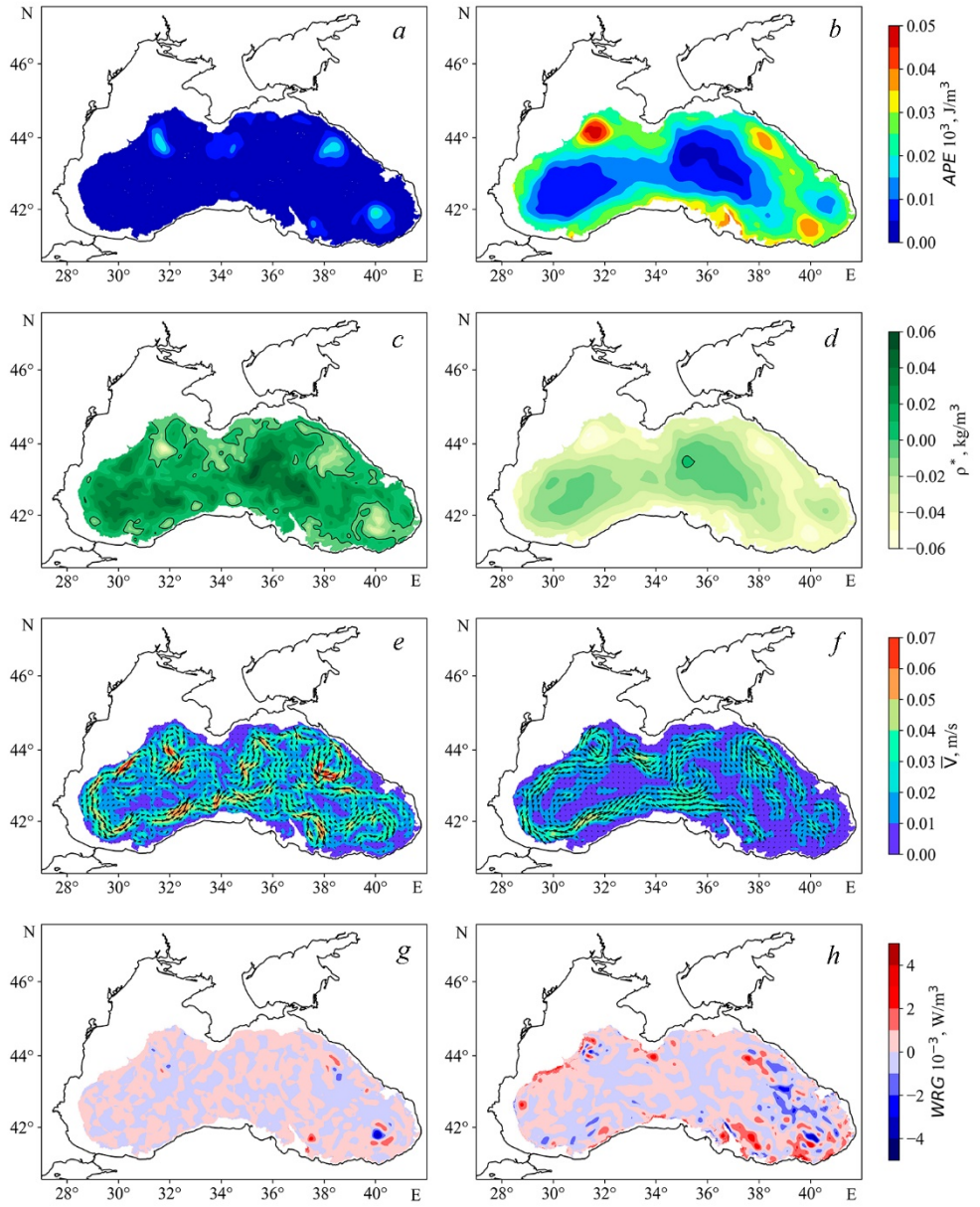

F i g. 4. Spatial distributions of *APE* (*a*, *b*), density anomaly (*c*, *d*), current velocities (*e*, *f*) and buoyancy work (*g*, *h*) at the 500 m depth based on the results of experiments 1 (*a*, *c*, *e*, *g*) and 2 (*b*, *d*, *f*, *h*) on June 15, 2016

At the deep horizons in summer (Fig. 4, *a*, *b*), the differences in the APE value are more significant than in the upper layer: firstly, the APE extremes in experiment

2 are approximately 2.5 times greater than in experiment 1; secondly, there is a significant difference in the APE value between the periphery and the central part of the sea. Comparison with the density anomaly fields shows that the increase in APE in experiment 2 is due to large absolute values of the density anomaly at the basin periphery (Fig. 4, *d*), whereas in experiment 1 the largest values are located in the center (Fig. 4, *c*). As shown in [19], such a structure of the APE fields and the density anomaly at the deep horizons is determined by mesoscale eddy variability. According to Fig. 4, *e* and *f*, the anticyclonic eddies near the continental slope have a clearer structure and their location coincides with the increased APE values in experiment 2. In addition, the analysis of the APE budget components showed that the contribution of the buoyancy work in the eddy zone increases in experiment 2 (Fig. 4, *h*).

For winter period, it was found that the greatest differences between the APE values in the two experiments were observed in the 40–100 m layer (Fig. 2, *b*). To identify their causes, the maps of the APE fields and density anomalies at the 50, 75, and 100 m horizons were analyzed. In accordance with Fig. 5, increased APE values are observed on the periphery of the basin in the western part of the sea in experiment 1 (Fig. 5, *a*) and these areas correspond spatially to the negative density anomalies (Fig. 5, *c*) in anticyclonic eddies. It is also evident that the spatial structure of the density anomaly fields in experiment 2 (Fig. 5, *d*) is significantly different from the experiment 1 data (Fig. 5, *c*).

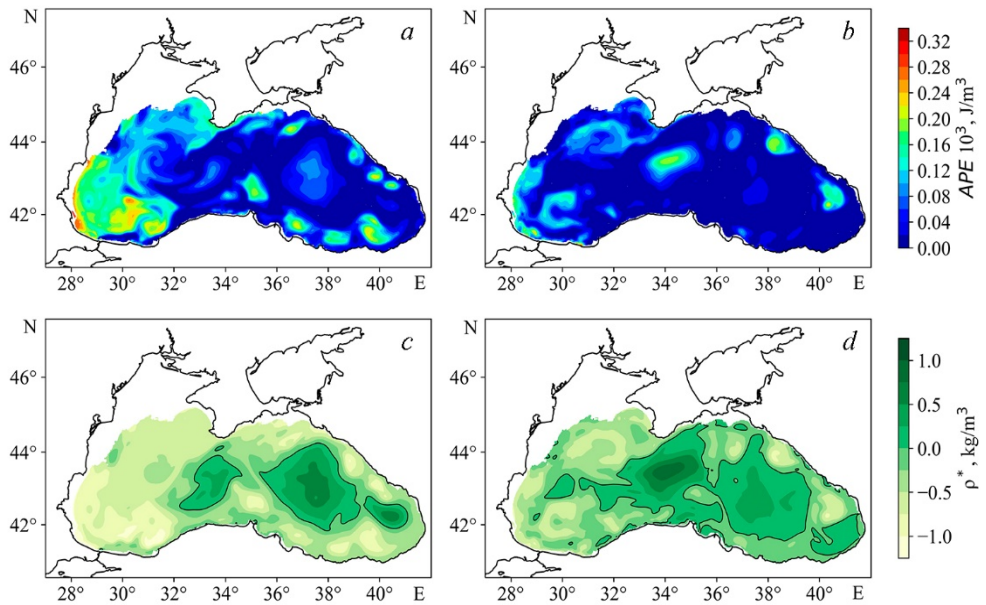

F i g. 5. Spatial distributions of *APE* (*a*, *b*) and density anomaly (*c*, *d*) at the 75 m depth based on the results of experiments 1 (*a*, *c*) and 2 (*b*, *d*) on December 15, 2016

Therefore, an additional estimate of the change in the temperature and salinity deviations over time from the measurement data for the southwestern part of the sea at the 50–100 m depths was carried out in winter. Three Argo profiling floats Nos. 3901852, 3901854, 3901855 were considered (the map of locations of the profiling stations is shown in Fig. 6, *a*). Fig. 6, *b* and *c* shows the model data deviations from those measured at the 75 m horizon. The average temperature deviation for 22.10.2016–28.12.2016 was −1.7 and +0.1 °C; the salinity deviation was 0.5 and 0.3‰ for experiments 1 and 2, respectively. As can be seen for the indicated floats in experiment 2, the deviations of the thermohaline characteristics decrease, therefore, the data are simulated more accurately than in experiment 1. Thus, for the winter season of 2016, the APE estimates obtained using the approximation schemes (2), (3) are more adequate to the real energy of the circulation.

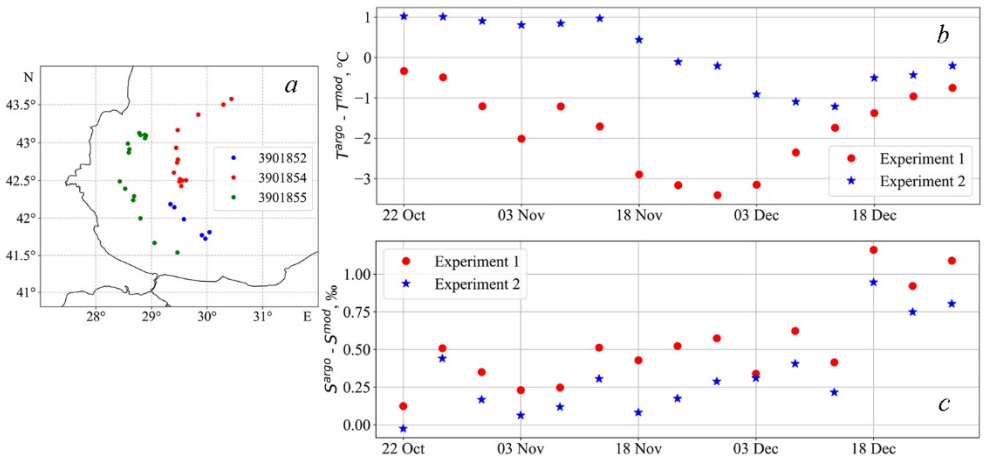

F i g. 6. Map of the locations of Argo profiling float stations (*a*), deviations of model temperature (*b*) and salinity (*c*) from the observation data at the 75 m depth in October–December 2016

For deep horizons in winter, the APE field structure is similar to that in summer, and increased values in experiment 2 are also observed on the basin periphery and by approximately two times exceed the experiment 1 data.

Conclusion

Based on the 2016 data, the paper analyses numerically the APE store and its budget components in the Black Sea obtained using a new scheme of temperature and salinity approximation in the advective transport operator for the heat and salt advection–diffusion equations in the MHI model (experiment 2). A comparison of the energy characteristics of the circulation is performed with the estimates obtained earlier based on the traditional approximation scheme (experiment 1). Differences in both integral values and spatial distribution of APE, buoyancy work and horizontal diffusion are obtained. It is found that the APE store in experiment 2 is 30%, on average per year, greater than in experiment 1. Moreover, in warm period, this

difference results from horizontal diffusion decrease, and in cold period, it is conditioned by a decrease in the APE amount spent on transformation into kinetic energy due to the buoyancy work.

As the analysis showed, the quantitative and qualitative discrepancies in the distributions of APE and its budget components between the results of the two experiments are due to differences in the fields of seawater density anomalies. In experiment 2 in the summer of 2016, the APE store in the upper layer was smaller than in experiment 1 due to a decrease in the density anomaly module on the NWS, and in winter, on the contrary, it was higher due to the formation of extensive areas of negative density anomalies in the western part of the sea corresponding to anticyclonic eddy formations. Throughout the year, the increased APE values below the 100 m horizon compared to experiment 1 are associated with an increase in density anomalies near the continental slope due to the intensification of mesoscale eddies.

As the validation of model thermohaline fields demonstrated, the use of the approximation scheme (2) permits a more accurate reproduction of salinity, and hence density, thus providing a more correct APE calculation in the Black Sea upper layer. Below the 300 m horizon, no significant discrepancies between the temperature and salinity in two calculations and observational data were found; but significant qualitative and quantitative differences were revealed for the energy characteristics: in experiment 2, the difference in APE values in the central part and on the basin periphery increases and the area of zones of extreme buoyancy work values increases.

According to the results of the study, the change in the model temperature and salinity associated with the new scheme for calculating the advective transfer of heat and salt causes a change not only in the density and APE, but also in the budget terms describing diffusion processes. The analysis showed that the areas of decreasing energy flux due to horizontal diffusion spatially correspond to the zones of decreasing horizontal salinity gradients. The indirect use of the new approximation scheme through a change in density helps to reduce the dissipation of available potential energy. It should also be noted that, according to preliminary estimates obtained in [9], a change in the temperature and salinity calculation scheme leads to an intensification of the upwelling of deep waters in the central part of the sea. Therefore, a change in advection affects vertical mixing and deep convection, however, this issue is beyond the scope of the presented work and is planned as a topic for a separate study.

The results obtained are useful for the analysis of the mechanisms of evolution of mesoscale eddies based on the estimate of the energy contributions of such physical processes as dissipation, instability, buoyancy work and pressure.

REFERENCES

1. Kamenkovich, V.M., Koshlyakov, M.N. and Monin, A.S., eds., 1986. *Synoptic Eddies in the Ocean*. Dordrecht: Springer, 444 p. https://doi.org/10.1007/978-94-009-4502-9

2. Gill, A.E., 1982. *Atmosphere – Ocean Dynamics*. New York: Academic Press, 662 p. https://doi.org/10.1016/s0074-6142(08)x6002-4

3. Von Storch, J.-S., Eden, C., Fast, I., Haak, H., Hernandez-Deckers, D., Maier-Reimer, E., Marotzke, J. and Stammer, D., 2012. An Estimate of the Lorenz Energy Cycle for the World Ocean Based on the 1/10° STORM/NCEP Simulation. *Journal of Physical Oceanography*, 42(12), pp. 2185-2205. https://doi.org/10.1175/JPO-D-12-079.1

4. Guo, Y., Bishop, S., Bryan, F.O. and Bachman, S., 2022. A Global Diagnosis of Eddy Potential Energy Budget in an Eddy-Permitting Ocean Model. *Journal of Physical Oceanography*, 52(8), pp. 1731-1748. https://doi.org/10.1175/JPO-D-22-0029.1

5. Cronin, M. and Watts, D.R., 1996. Eddy-Mean Flow Interaction in the Gulf Stream at 68°W. Part I: Eddy Energetics. *Journal of Physical Oceanography*, 26(10), pp. 2107-2131. https://doi.org/10.1175/1520-0485(1996)026<2107:EFIITG>2.0.CO;2

6. Yang, H., Chang, P., Qiu, B., Zhang, Q., Wu, L., Chen, Z. and Wang, H., 2019. Mesoscale Air-Sea Interaction and Its Role in Eddy Energy Dissipation in the Kuroshio Extension. *Journal of Climate*, 32(24), pp. 8659-8676. https://doi.org/10.1175/JCLI-D-19-0155.1

7. Holland, W.R., 1975. Energetics of Baroclinic Oceans. In: NAS, 1975. *Numerical Models of Ocean Circulation: Proceedings of a Symposium Held at Durham, New Hampshire, October 17–20, 1972*. Washington: National Academy of Sciences, pp. 168-177.

8. Demyshev, S.G., 2022. Discrete Equation for the Available Potential Energy as an Exact Consequence of the Numerical Model Equations. *Physical Oceanography*, 29(3), pp. 221-236. https://doi.org/10.22449/1573-160X-2022-3-221-236

9. Demyshev, S.G., 2023. Nonlinear Invariants of a Discrete System of the Sea Dynamics Equations in a Quasi-Static Approximation. *Physical Oceanography*, 30(5), pp. 523-548.

10. Demyshev, S.G. and Dymova, O.A., 2023. [Estimates of the Available Potential Energy Budget in the Black Sea Using New Approximation Schemes for the Heat and Salt Advection-Diffusion Equations]. *Multiphase Systems*, 18(4), pp. 378-381. https://doi.org/10.21662/mfs2023.4.117 (in Russian).

11. Demyshev, S.G. and Dymova, O.A., 2022. Analysis of the Annual Mean Energy Cycle of the Black Sea Circulation for the Climatic, Basin-Scale and Eddy Regimes. *Ocean Dynamics*, 72(3-4), pp. 259-278. https://doi.org/10.1007/s10236-022-01504-0

12. Mellor, G.L. and Yamada, T., 1982. Development of a Turbulence Closure Model for Geophysical Fluid Problems. *Reviews of Geophysics*, 20(4), pp. 851-875. https://doi.org/10.1029/RG020i004p00851

13. Simonov, A.I. and Altman, E.N., eds., 1991. *Hydrometeorology and Hydrochemistry of Seas in the USSR. Vol. IV. Black Sea. Issue 1. Hydrometeorological Conditions*. Saint Petersburg: Gidrometeoizdat, 428 p. (in Russian).

14. Nardelli, B.B., Tronconi, C., Pisano, A. and Santoleri, R., 2013. High and Ultra-High Resolution Processing of Satellite Sea Surface Temperature Data over Southern European Seas in the Framework of MyOcean Project. *Remote Sensing Environment*, 129, pp. 1-16. https://doi.org/10.1016/j.rse.2012.10.012

15. Arakawa, A. and Lamb, V.R., 1981. A Potential Enstrophy and Energy Conserving Scheme for the Shallow Water Equations. *Monthly Weather Review*, 109(1), pp. 18-36. https://doi.org/10.1175/1520-0493(1981)109<0018:APEAEC>2.0.CO;2

16. Bayankina, T.M., Godin, E.A., Zhuk, E.V., Ingerov, A.V., Isaeva, E.A. and Vetsalo, M.P., 2021. Information Resources of Marine Hydrophysical Institute, RAS: Current State and Development Prospects. In: T. Chaplina, ed., 2021. *Processes in GeoMedia* – Volume II. Cham: Springer, pp. 187-197. https://doi.org/10.1007/978-3-030-53521-6_22

17. Ivanov, V.A. and Belokopytov, V.N., 2013. *Oceanography of the Black Sea*. Sevastopol: ECOSI-Gidrofizika, 210 p.

18. Demyshev, S., Dymova, O. and Miklashevskaya, N., 2022. Seasonal Variability of the Dynamics and Energy Transport in the Black Sea by Simulation Data. *Water*, 14(3), 338. https://doi.org/10.3390/w14030338

19. Bulgakov, S.N. and Korotaev, G.K., 1984. Possible Mechanism of Stationary Circulation of Black Sea Waters. In: MHI, 1984. *Integrated Research of the Black Sea*. Sevastopol: MHI, pp. 32-40 (in Russian).

Submitted 27.03.2024; approved after review 17.04.2024;
accepted for publication 17.08.2024.

About the author:

Olga A. Dymova, Leading Researcher, Marine Hydrophysical Institute of RAS (2 Kapitanskaya Str., Sevastopol, 299011, Russian Federation), CSc. (Phys.-Math.), **ORCID ID: 0000-0003-4036-2447**, **ResearcherID: P-9669-2015**, **Scopus Author ID: 6508381809**, olgdymova@mhi-ras.ru

The author has read and approved the final manuscript.
The author declares that she has no conflict of interest.